Proceedings of the ASME 2022 41st International Conference on Ocean, Offshore and Arctic Engineering
OMAE2022
June 5-10, 2022, Hamburg, Germany

OMAE2022-79203

A STATISTICAL MODEL OF MOTION MAXIMA OF OFFSHORE WIND TURBINE COMPONENTS DURING INSTALLATION

Lena Ströer *
University of Bremen
Bremen, Germany
Email: l.stroeer@uni-bremen.de

Andreas F. Haselsteiner
University of Bremen
Bremen, Germany
Email: a.haselsteiner@uni-bremen.de

Aljoscha Sander
University of Bremen
Bremen, Germany
Email: alsander@uni-bremen.de

Klaus-Dieter Thoben
University of Bremen
Bremen, Germany
Email: thoben@uni-bremen.de

ABSTRACT

Single blade installation presents a significant challenge in the installation of offshore wind turbines. The stochastic nature of wind speed and wave height lead to uncertainties during installation. Blade installation is especially difficult in the presence of large relative motions between the blade root and the hub of the nacelle. In a measurement campaign, the installation of the Trianel Windpark Borkum II wind farm was analyzed to better understand installation difficulties. Sensor boxes recorded acceleration and GPS signals. In the study presented here, the oscillating behavior of the tower and the single blade installation tool (SBIT) before the first contact with the tower based on the data of the measurement campaign was described. Statistical models were developed to investigate how turbine and tool move conditional on wind and wave parameters. These statistical models describe the maximum deflection in blocks of 1 minute conditional on wind and wave parameters. The 1 minute block maxima are represented by a generalized extreme value distribution. We found that the oscillations of the tower are much higher than the oscillations of the SBIT. Thus, they seem to determine the process of the single blade installation. The developed model for tower motion maxima uses wind speed and significant wave height as covariates. While these relationship explain some of the variability of observed motion maxima, much uncertainty remains, which cannot be explained by correlations with wind speed and wave height. Nevertheless, we hope that the turbine's model can be used to improve the quality of the decision of whether current environmental conditions are suitable to install the rotor blade or whether one should wait for better weather.

INTRODUCTION

Various factors have been pushing the growth of the renewable energy sector. The European Commission predicts that onshore and offshore wind energy together will account for half of Europe's electricity by 2050 with a capacity rising from 220 GW today up to $1,300$ GW [1]. In the past years the limited space on land, the competing site usage, the less general environmental impact, and the higher wind resource offshore stimulated the technology of offshore wind energy [2]. The constantly increasing size of wind turbines are an efficient and economical choice from an operational point of view, however this involves higher challenges and risks during the transportation and installation of these turbines [3]. The components of a wind turbine, especially the rotor blades are very sensitive and small damages can lead to high costs. Any damage to the root connection implicates bringing the lifted rotor blade back to the deck of the installation ves-

*Address all correspondence to this author.

sel. A delay in the installation task causes the loss of favorable weather windows and thus high financial cost due to a longer utilization of the installation vessel. Hence, during transportation and installation, a high precision is required.

The possibilities to carry out research during offshore wind turbine (OWT) installation are rare. This is due to the limited access to offshore wind farms and the linked costs. Hence, only a few on-site experiments investigating the process of the installation have been conducted (e.g. [4], [5] [6] [7]). The study of Oelker et al. (2021), showed that a tuned mass damper could be a cost-effective tool to improve the process of single blade installation in general [7]. Generally, different installation concepts of OWTs exist and different pre-assembly strategies are described in the literature, e.g. "rotor-star" or "bunny-ear" assembly [8] [9] [7]. Among the commonly used installation methods for offshore wind turbines, the single blade installation was most frequently used in recent years, due to small deck space requirement and flexible blade orientations during installation [10]. The numerical studies of Verma et al. (2019) [11], Jian et al. (2018) [12], Verma et al. (2021) [13] and Ren et al. (2018) [14] investigated the behavior of the turbine during single blade installation numerically. In these studies, it was found that wind-induced loads dominate the motions of the blade and wind- and wave-induced loads dominate the motions of the tower. These factors significantly limit the installation of blades [11] [12] [13] [14]. The blade landing process can be challenging if large relative motions appear between the blade root and the hub of the nacelle. Verma et al. (2019) [11] presented a probability-based methodology to assess limiting sea states for single blade installation using response-based criteria. In the following, this serves as an inspiration for the task of this study. In the publication of Verma et al. (2019) [11], the allowable sea states for the mating phase of blade and hub are estimated. An extreme value analysis of the limiting response parameter has been performed.

Sander et al. (2020) found, that tower vibrations of partially installed turbines can be well described as a sequence of evolving ellipses [5]. In a novel experiment a torsional coupling mechanism linking motions in the fore-aft and side-side direction was presented which explains the formation of orbits that change its direction [15]. In latest research, it has been found that the tower oscillations and the resulting deflections determine whether the blades can be mounted. The influence of the SBIT movements has not been further considered and it is assumed that the turbine dominates the installation procedure [5] [6]. However, yet, no study has proven that motion maxima of the SBIT do not influence the success of the installation. Furthermore, it is unclear how motion maxima of both the tower and the SBIT change with environmental conditions. Thus, it is difficult to plan the installation of offshore wind turbines precisely.

Based on measured accelerations of the blade lifting device and the turbine's nacelle during a measurement campaign of the wind farm Trianel II [5] [6] in combination with the environmental conditions wind speed (V) and wave height (H_s), we now seek to determine the exact behavior of the SBIT and tower during installation. Here, we pursue the approach of a statistical model describing the motion maxima of the tower and SBIT during single blade installation conditional on wind speed and wave height. We aim to enable better planning of the offshore operation through a statistical model of the turbine's and SBIT's deflection during installation. The model describes motion maxima of "independent sequences" of turbine and SBIT oscillations meaning that we only consider time series before any collisions occurred. Based on these independence sequences, statistical models of the environmental conditions and the turbine response are developed in order to predict the turbine dynamics during installation.

DATA AND METHODS

Datasets

As part of a measurement campaign, the installation of the Trianel Windpark Borkum II wind farm was measured to better understand the installation difficulties. During this measurement campaign, sensor boxes were installed on various components of the wind turbines during installation, including on the blade lifting device used for single blade installation. During each installation, one sensor box was placed at the helicopter hoisting platform of the turbine and two other boxes were placed at the SBIT tip and SBIT root (figure 1). These sensor boxes recorded acceleration and GPS signals. The technical specifications of the turbines and the measurement boxes are published in Sander et al. (2020) [5] [6]. Additionally, a LIDAR (light detection and ranging device) installed on the installation jack-up unit, provided wind field measurements and a wave buoy close to the installation site collected wave data including e.g. significant wave height, peak period and wave direction [6].

In figure 2 the environmental data set which will be used in this study is compared to a metocean data set used in a recent benchmark study on estimating offshore environmental conditions [16]. All metocean data sets used in the benchmark study show the characteristic dependency of the wave height on the wind speed as presented in figure 2. The environmental data set used in the subsequent analyses does not exhibit these characteristics. The measurement data set only seems to represent a fraction of the typical wind speed-wave height space. However, it is found that even if the data set does not follow the typical dependency, it does represent the lower wind speeds and wave heights of the metocean data set. This is explicable with the restricted selection of environmental conditions during the installation of the rotor blades.

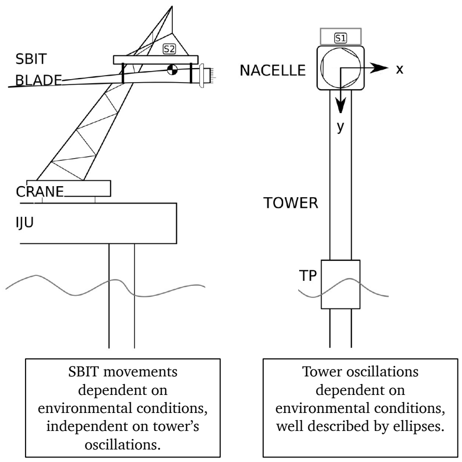

FIGURE 1. Single blade installation at wind farm Trianel II altered after Sander et al. (2020) and Sander et al. (2020a) [6] [5]. S1 and S2 are the two sensor boxes that were used to track the motions of the tower and the single blade installation tool (SBIT).

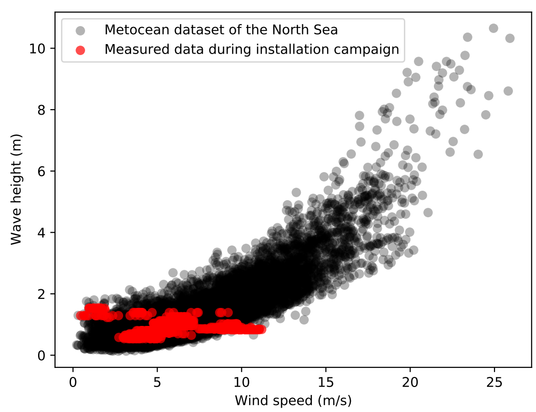

FIGURE 2. Scatter plot comparing the wind speed and wave height measured during the installation of the Trianel Windpark Borkum II wind farm to environmental data recently used in a benchmark study on estimating offshore environmental conditions [16].

Data availability

For this study, we created an own zenodo repository, where the utilized and processed data sets of the measurement campaign together with our codes are published open access [17]. The original data recorded during the installation of the Trianel Windpark Borkum II wind farm are published open access on another zenodo repository [18].

Independent oscillations

We consider only "independent oscillations" for our model that represent the state when the blade is lifted to the height of the nacelle but no contact between blade and nacelle occurred yet. The end of an independent oscillation could be either the successful blade landing or an impact event of SBIT and tower. Since most installation attempts do not proceed straightforward without any impact, the end of an independent oscillation usually is an impact of SBIT and tower. Hence, the first independent time sequence lasts from the start of the installation until the first impact. Knowing the blade landing times from the previous work of Holman (2021) [19], the individual installation periods of the rotor blades can be identified. Here, we define an individual installation period as the time from the start of installation (SBIT at hub height) until the successful mounting of the blade to the hub. Then, by identifying the impact events, the independent oscillation sequences can be determined. Due to the aerodynamically designed structure of the rotor blade and the SBIT (figure 1), environmental and impact loads cause pendulum oscillation motions at the blade root during the installation task [11]. To distinguish an impact event from a measurement error or a collision of the SBIT while being stored at the deck of the installation vessel, three general conditions need to be fulfilled:

1. The SBIT is at hub height. This condition ensures that the installation process has started.
2. The impact event has to last a certain time, to avoid counting measurement errors as impacts.
3. Between two consecutive impact events, there has to be a certain time difference. This condition ensures that the impact events do not correlate with each other.
4. The fourth and exclusive condition to identify an impact is the acceleration threshold above which impacts are distinguished from regular SBIT motions.

To determine the acceleration thresholds, we chose a simple approach and analyzed the time series of the SBIT acceleration of 3 turbines in x-, y-, and z-direction visually and tested different acceleration limits. Then, another algorithm has been developed that determines the independent oscillations by comparing the list of impact events with the installation period. The following conditions have to be fulfilled to clearly define independent sequences:

1. The impact event needs to be within the installation period of the blade.
2. The first impact event has to be further in time than the begin of the installation attempt.
3. The first impact has to be the first in a series of impact events after the begin of the corresponding installation period.

Reflecting on the impact algorithm it can be said, that it failed to identify all moments in time where the rotor blade and tower have been connected to each other. As a consequence, we manually filtered the data set a second time to ensure an independent data set of SBIT and tower oscillations and environmental conditions.

Extreme event extraction

Here, we are interested in maxima – extremes – of the deflection (d) time series (figure 4). These large displacements from the the origin of the tower and the SBIT are caused by environmental phenomena and could evoke an interruption or failure of the installation process. Extremes of subsamples (blocks) of a data set can be described with the generalized extreme value distribution [20] [21]:

$$F(x) = \begin{cases} \exp\left(-\exp\left(-\frac{x-\mu}{\sigma}\right)\right), \zeta = 0, \\ \exp\left(-\left(1+\zeta\frac{x-\mu}{\sigma}\right)_+^{-1/\zeta}\right), \zeta \neq 0. \end{cases} \tag{1}$$

To determine the statistical distribution of extreme events, the peaks in the data have to be identified. Given the case that the stochastic process is time correlated, it needs to be assured that each peak corresponds to an independent extreme event. In this study, we applied the block maxima method. A straightforward approach to filter out independent peaks in a data set is to make sure that the time difference between selected peaks is sufficient. When applying the block maxima method with a sufficiently wide block length, this criterion is fulfilled [22]. Applying this method, the data set is divided into a set of sequences (blocks) of equal length. Then, the largest peak of each block is extracted. When it cannot be assured that the data points are uncorrelated, an additional condition needs to be fulfilled to make sure that the peaks are uncorrelated. A common method is to make sure that the time difference between the peaks is greater than the autocorrelation length. Fogle et al. (2008) found that the maxima of $40-60$ seconds blocks can be considered independent when analyzing wind turbine load responses [23].

The short-term turbine response during the installation will be described by the individual peak deflections of the SBIT and tower (d_{max}). The time series of deflections will form 1-minute blocks of which block maxima will be described (see figure 4). This results in the short-term dynamics described by several blocks which contain the motion maxima. These block maxima have less serial correlation and will be described with a statistical model.

Figure 3 shows the distribution of the block maxima of the SBIT and the tower as well as the considered environmental conditions. Generally, it is found, that neither parameter strongly correlates with another parameter. Hence only part of the variability of motion maxima during installation can be explained by correlations with wind speed and wave height. Note, that this phenomenon adds uncertainty to the statistical models developed in this study. Table 1 shows the linear correlation coefficients of the tower's and SBIT's peak deflections.

TABLE 1. Overall linear correlation (correlation coefficient r) between environmental parameters and the peak deflection of SBIT and tower.

Linear correlation	V	H_s	d_{tower}	d_{SBIT}
Wind speed	1	0.078	0.205	0.148
Wave height	0.078	1	0.096	0.247
Tower deflection	0.205	0.096	1	0.095
SBIT deflection	0.148	0.247	0.095	1

Statistical model of motion maxima

The statistical approach in this work is inspired by the environmental model in the work of Mackay et al. (2020) [24] and the response model in the work of Haselsteiner et al. (2021) [25]. We model the distribution block maxima and how they depend on environmental variables using parametric dependence functions. Then we develop two separate statistical models since we analyze the deflections of the tower and the SBIT individually. Consequently, the two statistical models presented here describe the response of the tower and the SBIT conditional on the environmental variables wind speed and wave height. That implies for given environmental conditions, the deflection of the SBIT and tower can be determined.

RESULTS AND DISCUSSION

Statistical model of the SBIT's motion

For our model the response of the SBIT during single blade installation, we assumed, that the oscillations of the SBIT are only conditional on wind parameters. Calculating the linear correlation coefficient between wind speed and deflection resulted in $r = 0.148$ (table 1). Hence, interpreting this correlation coefficient, it can be said, that the linear relationship between the SBIT's peak deflection and the wind speed is rather week. Nevertheless, when analyzing the lowest scatter points in figure 5, one could suppose that the minimum peak deflections are increasing linearly with the wind speed.

Calculating the correlation coefficient of the minimum peak deflection and intervals of the 1 - minute mean wind speed resulted in $r_{min} = 0.764$. While the correlation coefficient of all peak deflections and wind speed indicates a weak correlation, this correlation coefficient points at a rather high linear correlation (figure 5). Nevertheless, the suspected linear dependency be-

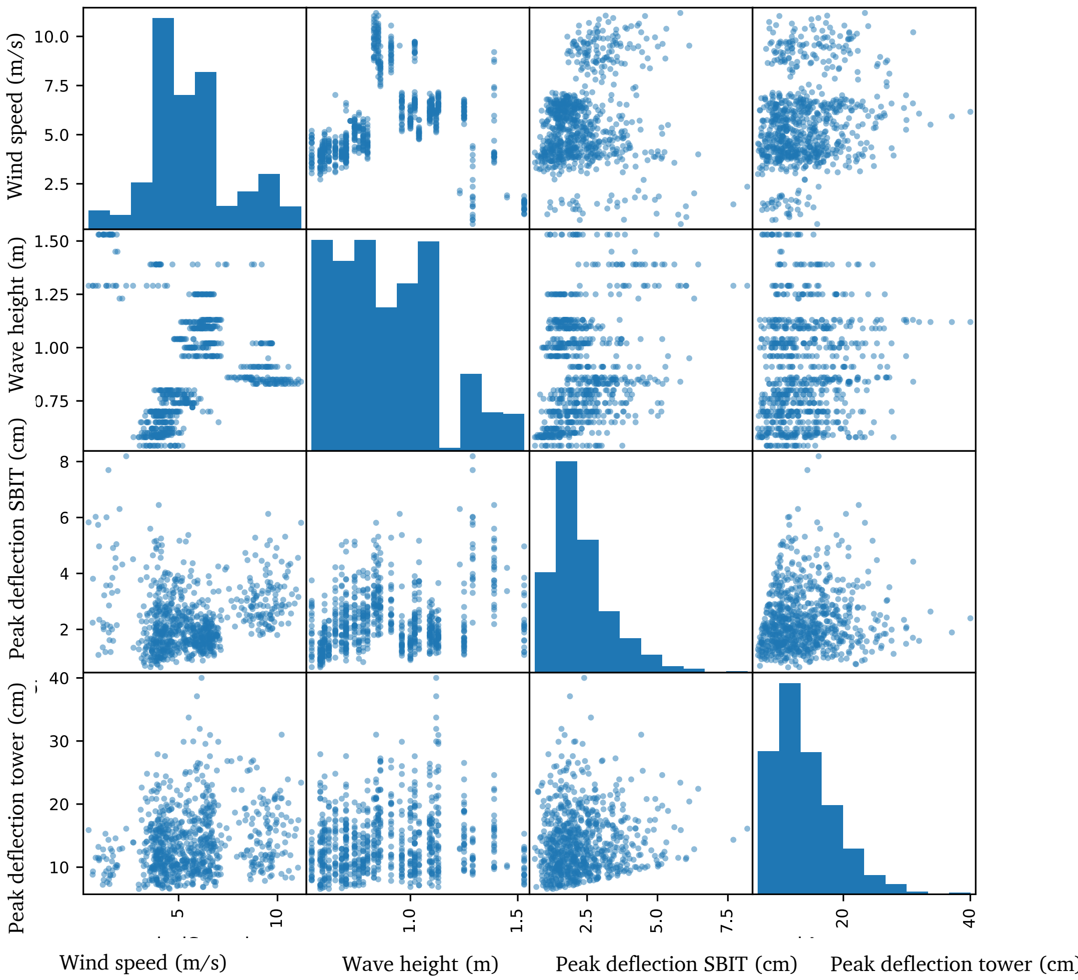

FIGURE 3. Scatter plot matrix of the peak deflections of SBIT and tower and the corresponding environmental conditions.

tween minimum peak deflection and wind speed is not sufficient to describe the behavior of the SBIT during single blade installation. Especially the highest peak deflections are scattered which increases the uncertainty and the complexity of modelling the dependency (figure 5). In general, there are two possible ways to interpret the results presented above. The first interpretation would confirm the assumption of the SBIT's oscillations not being strongly dependent on the wind speed. A statistical model of the SBIT's deflections conditional on the wind speed would thus have little significance. The second interpretation would imply questioning the reliability of the applied impact identification algorithm. Probably, the highest peaks in the deflections, that are causing the highly scattered values at low and medium wind speeds are impact events that have not been detected by the impact algorithm.

Calculating the linear correlation between the individual parameters of the GEV distribution and the wind speed showed that the shape, location and scale parameters and the wind speed are medium linearly correlated (table 2).

TABLE 2. Comparison of the correlation between the different parameters of the GEV distribution describing the motion maxima of the SBIT and the wind speed.

	Correlation coefficient r
Shape ζ	0.597
Location μ	0.476
Scale σ	-0.534

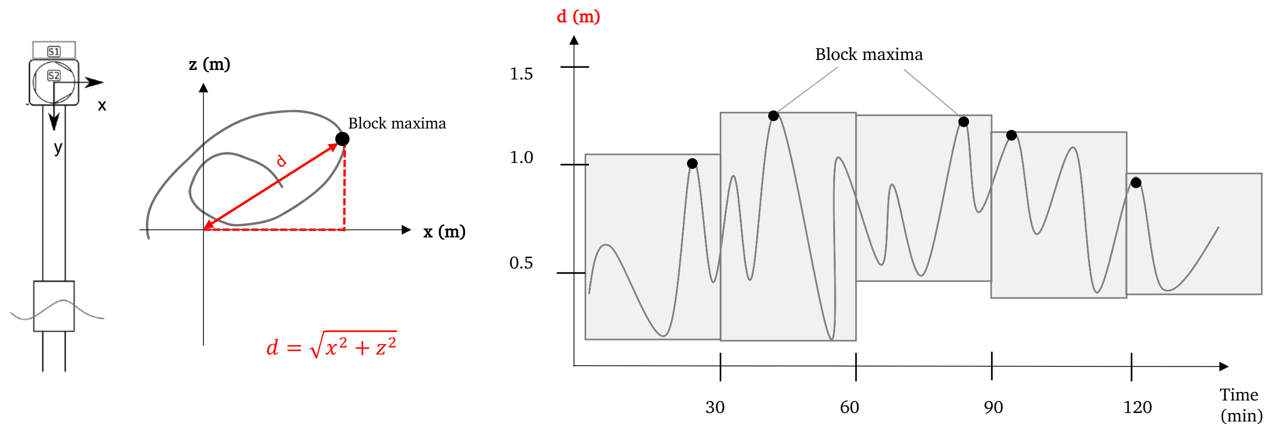

FIGURE 4. The models use maxima of 1-minute blocks of the deflection.

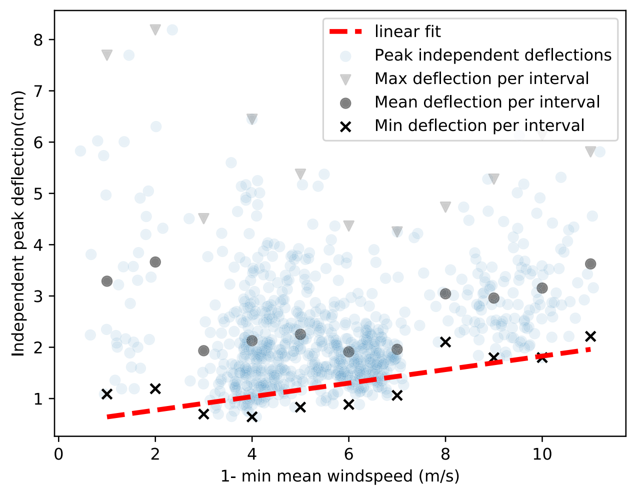

FIGURE 5. Minimum peak deflections of the SBIT over the 1-minute mean wind speed.

SBIT motion conditional on wind speed Here, we present a statistical model which consists of the SBIT's response during installation and the environmental variable wind speed. Although the correlation coefficients presented in table 2 are not indicating a strong linear dependency, we fitted simple linear functions to the intervals of wind speed and the parameters of the GEV distribution. Figure 5 suggests that the deflection of the SBIT increases with the wind speed. Thus, it seems to be physically reasonable that the distribution of the deflection is shifted with increasing wind speeds. Therefore, we assume, that the location parameter, which is responsible for the shift of a distribution, increases linearly with the wind speed. To keep model complexity low, we decided to use the fixed values of the global GEV distribution, which have been calculated above for the shape and scale parameter ($\zeta = -0.143$ and $\sigma = 0.697$). The location parameter of the statistical model of the SBIT's response is described by a linear function of the wind speed:

$$\mu(v) = a_1 v + a_2 \tag{2}$$

The parameters are estimated to be $a_1 = 0.089$ and $a_2 = 1.676$ by using the method of least squares and the python package virocon [26]. Consequently, the statistical model of the SBIT's deflection consists of two fixed values for the shape and scale parameters of the GEV distribution and two parameters resulting from the linear dependency of the location parameter and the wind speed.

Analyzing the model quantitatively, different quantiles of the measurement data and the statistical model are compared (figure 6). It is found that the model represents the deflection of the SBIT fairly reasonable. Excluded from this observation is the drop of deflections at wind speeds around $4-8$ m/s, when analyzing the 90 th percentile of the data. Additional research is necessary, investigating this phenomenon.

With the statistical model for the SBIT's response, it is possible to make a statement of the expected deflections of the SBIT for different wind speeds. Nevertheless, one needs to take into account that modeling the location parameter as a linear function of the wind speed and including this function into the statistical model involves uncertainty, since the correlation coefficient only indicates a medium linear correlation between the location parameter of the GEV distribution and the wind speed. Given that the critical deflection of the SBIT above which an installation is interrupted is known, the installation crew can read the critical wind speed until which the installation can be carried out. Finally, we point to the dimensions of the structure and the 90th percentile of the peak deflections of the SBIT (figure 6). The

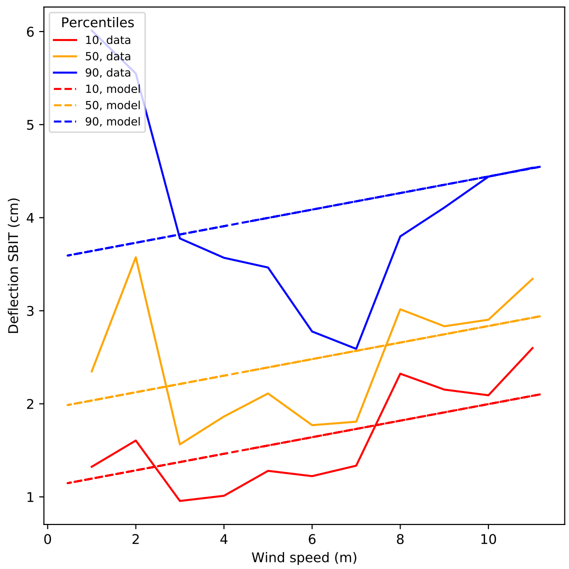

FIGURE 6. Percentile curves of the empirical joint distribution of the SBIT's deflection and wind speed (measurement data) and the statistical model.

highest peak deflections of the SBIT only reach a maximum 6 cm which is much smaller than the tower's motion.

Statistical model of the tower's motion

Here, we present two statistical models which consists of the tower's response during installation and the environmental variables wave height and wind speed. Similar to the response model of the SBIT, the response emulator of the tower is also designed as a GEV distribution. The shape, location and scale parameters (ζ, μ, σ) are modeled as parametric functions of the wind speed and wave height.

As a next step, the linear correlation between the parameters of the GEV distribution and intervals of the wind speed and wave height have been calculated. The results in table 3 indicate, that the location parameters are strongly linear dependent on the wind speed and the wave height. However, the shape parameter does not correlate with either environmental variable while the scale parameter only correlates with the wind speed.

Tower's motion conditional on wave height With the findings presented above, we decided to first build a simple response model which describes the peak deflections of the tower conditional on the wave height (model A). Both, the scale and shape parameter only show a weak linear correlation (table 3). Hence, only the location parameter of the GEV distribution is described as a linear function of the wave height. The scale and shape parameter are modeled as fixed values taken from the

TABLE 3. Comparison of the correlation (correlation coefficient r) between the different parameters of the GEV distribution and intervals of the wind speed and wave height.

	r wind speed	r wave height
Shape ζ	0.173	-0.042
Location μ	0.882	0.801
Scale σ	0.713	-0.429

global GEV distribution of the peak deflections of the tower: $\zeta = -0.122$, $\sigma = 3.397$. The location parameter is described as a linear function of the wave height:

$$\mu(h_s) = b_1 h_s + b_2 \tag{3}$$

The parameters were estimated as $b_1 = 1.987$ and $b_2 = 9.733$ using the method of least squares and the python package virocon [26]. Consequently, the model consists of two fixed values for the shape and scale parameters of the global GEV distribution and two parameters resulting from the linear dependency of the location parameter and the wave height. In their analyses, Verma et al. (2019) [11] found that the wave parameters are essential for estimating limiting sea states since these parameters significantly influence the monopile oscillations during the blade-root mating task. However, analyzing the linear correlation coefficient, the influence of the wind speed on the location parameter of the GEV distribution is higher. Therefore, by ignoring the fact of higher correlation with the wind speed, we accept a higher uncertainty of model A in general. The model's quality is reviewed by a quantitative analysis in the following.

Tower's motion conditional on wave height and wind speed The second model for the tower consists of the turbine's response during installation and the two environmental variables wave height and wind speed (model B). When analyzing the correlation coefficients in table 3, it is seen that the shape parameter is dependent on neither environmental parameter. Therefore, we modeled the shape parameter as a fixed value taken from the global GEV distribution presented above. The location parameter exhibits a high linear dependency on both the wave height and the wind speed. Hence, μ is modeled as a linear function of both environmental parameters. Geometrically, a 2-dimensional linear function means spanning a surface in the vector space of wave height, wind speed and the tower's deflection (equation 4). The scale parameter exhibits a linear dependency on the wind speed. Consequently, we describe the scale parameter as a linear function conditional on the wind speed.

TABLE 4. Fitted parameters of model B.

Parameter	Value
c_1	2.471
c_2	-0.076
c_3	9.322
c_4	0.395
c_5	1.589

A GEV distribution is fitted to each interval of wind speed-wave height combinations, describing the probability distribution of the tower's peak deflection for this specific interval of environmental conditions. As before, this results in one shape, location and scale parameter per interval. Calculating a linear function in the 3D variable space of wave height, wind speed and the location parameter implies fitting a plane equation of the form:

$$E = \left\{(x,y,z) \in \mathbb{R}^3 | z = ax + by + c\right\}. \tag{4}$$

To calculate the best fit linear plane for the location parameter conditional on the environmental parameters, scipy's linear algebra functions and the method of least-squares solution to an equation have been used. Here, by fitting a plane equation to the location parameter, the dependency on the wave height and wind speed is calculated at once. Hence, all parameters of model B have been fitted simultaneously. The scale parameter's function has been fitted using the method of least-squares and the python package virocon again. Consequently, model B consists of one fixed value for the shape parameter of the global GEV distribution ($\zeta = -0.112$) and five parameters resulting from the linear dependency of the location parameter on the wave height and wind speed and from the linear dependency of the scale parameter on the wind speed. The fitted parameters are indicated in table 4.

$$\mu(h_s, v) = c_1 h_s + c_2 v + c_3 \tag{5}$$

$$\sigma(v) = c_4 v + c_5. \tag{6}$$

Comparison of the models The presented models above could serve as an installation assistance, since they are able to describe the deflection of the tower during single blade installation. Analyzing the two models quantitatively, different quantiles of the measurement data and the two models are compared (figure 7). Here, to make the models comparable, we calculated the 10 th, 50 th and 90 th percentiles of the two models and the original data set. Analyzing the 10 th and 50 th percentile, it is found that the statistical model of the tower's deflection and the wave height predicts higher values for the peak deflection of the tower, compared to the statistical model of peak deflection, wave height and wind speed. For the 90 th percentiles the opposite is determined. The 10 th, 50 th and 90 th percentiles of the statistical models together with the corresponding percentiles of the measurement data are plotted in figure 7 and 8. Since the model of peak deflection and wave height does not include a dependency of the wind speed, the models can only be compared on the basis of the wave height. Based on the average of the mean absolute error (MAE), the two models provide equally good results ($MAE_A = 1.330$ and $MAE_B = 1.330$, table 5).

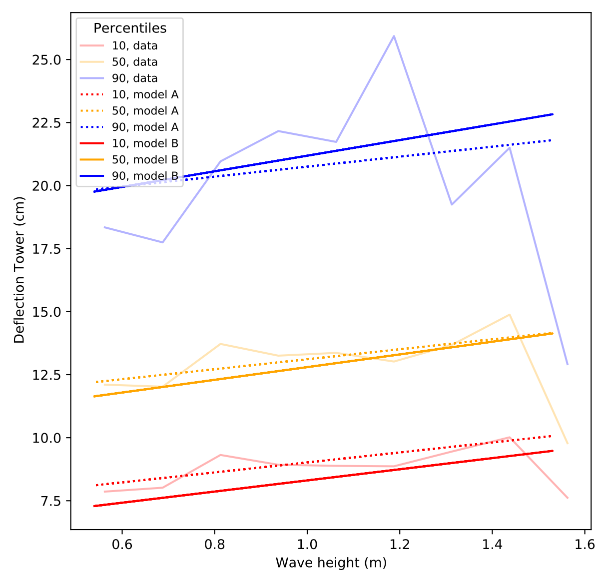

FIGURE 7. Percentile plot of model A and B of the tower and the measurement data in the wave plane.

CONCLUSION

For the installation process it is crucial to know the dependency of the peak deflections of SBIT and tower on the wave height and wind speed. We recommend to model the peak deflection of the SBIT as a GEV conditional on the wind speed. The peak deflection of the tower is modeled as a GEV distribution conditional on wave height and wind speed. Previous anal-

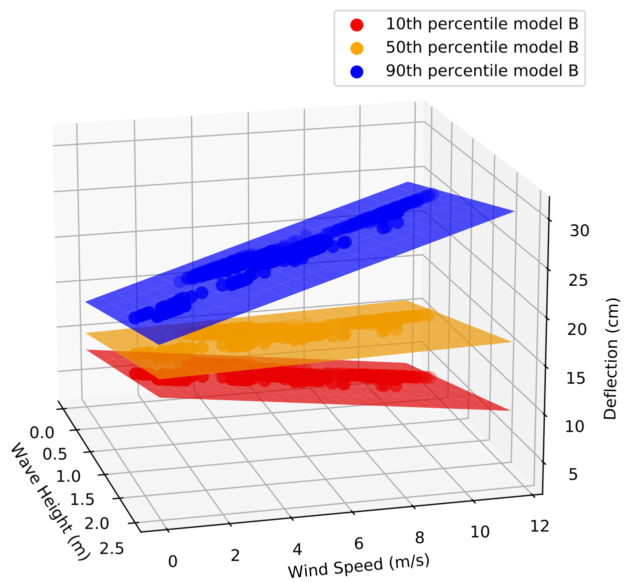

FIGURE 8. Percentiles of model B. Visualized as a 3D plane.

TABLE 5. Overview about the goodness of fit of the statistical models of the maximum deflections of SBIT and tower. * Note, that model A is stands for the statistical model of the tower's deflection given wave height. Model B stands for the model of the tower's deflection given wave height and wind speed.

	d_{max} SBIT (cm)	d_{max} tower (cm)
Data	6.00	25.00
Model	4.50	20.50 (model A*)
		22.50 (model B*)
Average MAE	0.54	1.33 (both models)

yses did not lead to clear evidence that the SBIT's oscillations are contributing to a successful or failed installation. Although we developed a model for the 1 - minute response of the SBIT and the tower during single blade installation, we did not find a strong indicator that the oscillations of the SBIT are significantly influencing the installation procedure (table 5). When comparing, for example the 90 th percentile of the SBIT's deflections to the tower's deflection (figure 6 and 7), it is found that the tower's deflections are over 4 times higher than the SBIT's deflections.

During wind turbine installation, we recommend to orientate on a high percentile such as the 90 th percentile of a model of 1 - minute peak deflection. Such a model allows the installation personnel to determine, at which environmental conditions the deflections of the tower are below critical values with a certain probability and risk. The present results do not allow to express a clear recommendation whether to use the SBIT's model in decision-making processes during single blade installation, hence, more research is required analyzing the motion of the SBIT during the blade root mating task. Moreover, studying the probability of occurrence of impact events and their correlation with deflections could complement the results of this study.

REFERENCES

[1] Wind Europe, 2021. Wind delivers the energy society wants. `https://windeurope.org/about-wind/wind-energy-today/`, accessed 22-10-2021.

[2] Esteban, M. D., Diez, J. J., López, J. S., and Negro, V., 2011. "Why offshore wind energy?". *Renewable Energy,* ***36***, pp. 444–450.

[3] Verma, A., Jiang, Z., Vedvik, N., Gao, Z., and Ren, Z., 2019. "Impact assessment of a wind turbine blade root during an offshore mating process". *Engineering Structures,* ***180***, pp. 205–222.

[4] Maes, K., De Roeck, G., and Lombaert, G., 2018. "Motion tracking of a wind turbine blade during lifting using RTK-GPS/INS". *Engineering Structures,* ***172***(0), pp. 285–292.

[5] Sander, A., Haselsteiner, A. F., Barat, K., Janssen, M., Oelker, S., Ohlendorf, J.-H., and Thoben, K.-D., 2020. "Relative motion during single blade installation: measurements from the north sea". In Proceedings of the 39th International Conference on Ocean, Offshore and Arctic Engineering, OMAE2020, ASME.

[6] Sander, A., Meinhardt, C., and Thoben, K.-D., 2020. "Monitoring of offshore wind turbine under wave and wind loading during installation". In XI International Conference on Structural Dynamics, EuroDyn 2020.

[7] Oelker, S., Sander, A., Kreutz, M., Ait-Alla, A., and Freitag, M., 2021. "Evaluation of the impact of weather-related limitations on the installation of offshore wind turbine towers". *Energies,* ***14***(13).

[8] Oelker, S., Ait-Alla, A., Lütjen, M., Lewandowski, M., Freitag, M., and Thoben, K.-D., 2017. "A Simulation Study of Feeder-Based Installation Concepts for Offshore Wind Farms". In The 27th International Ocean and Polar Engineering Conference, International Society of Offshore and Polar Engineers (ISOPE).

[9] Rippel, D., Jathe, N., Lütjen, M., Szczerbicka, H., and Freitag, M., 2019. "Integrated Domain Model for Operative Offshore Installation Planning Integrated Domain Model for Operative Offshore Installation Planning". In Digital Transformation in Maritime and City Logistics. Smart Solutions for Logistics., C. Jahn, W. Kersten, and R. C.M., eds., no. November, epubli GmbH, pp. 25–54.

[10] Zhao, Y., Cheng, Z., Sandvik, P. C., Gao, Z., and Moan, T.,

2018. “An integrated dynamic analysis method for simulating installation of single blades for wind turbines”. *Ocean Engineering,* ***152***(7491), pp. 72–88.

[11] Verma, A. S., Jiang, Z., Ren, Z., Gao, Z., and Vedvik, N. P., 2019. “Response-based assessment of operational limits for mating blades on monopile-type offshore wind turbines”. *Energies,* ***12***(10), pp. 1–26.

[12] Jiang, Z., Gao, Z., Ren, Z., Li, Y., and Duan, L., 2018. “A parametric study on the final blade installation process for monopile wind turbines under rough environmental conditions”. *Engineering Structures,* ***172***(April), pp. 1042–1056.

[13] Shankar Verma, A., Jiang, Z., Ren, Z., Caboni, M., Verhoef, H., van der Mijle-Meijer, H., Castro, S. G., and Teuwen, J. J., 2021. “A probabilistic long-term framework for site-specific erosion analysis of wind turbine blades: A case study of 31 Dutch sites”. *Wind Energy,* ***24***(11), pp. 1315–1336.

[14] Ren, Z., Jiang, Z., Gao, Z., and Skjetne, R., 2018. “Active tugger line force control for single blade installation”. *Wind Energy,* ***21***(12), pp. 1344–1358.

[15] Aljoscha Sander and Bas Holman and Andreas Haselsteiner, 2022. Could mass eccentricity explain the formation of orbits in wind turbines? `https://arxiv.org/pdf/2110.12802.pdf`, accessed 03-01-2022.

[16] Haselsteiner, A. F., Coe, R. G., Manuel, L., Chai, W., Leira, B., Clarindo, G., Soares, C. G., Hannesdóttir, Á., Dimitrov, N., Sander, A., Ohlendorf, J.-H., Thoben, K.-D., de Hauteclocque, G., Mackay, E., Jonathan, P., Qiao, C., Myers, A., Rode, A., Hildebrandt, A., Schmidt, B., Vanem, E., and Huseby, A. B., 2021. “A benchmarking exercise for environmental contours”. *Ocean Engineering,* ***236***.

[17] Ströer, L., 2021. Single blade installation of offshore wind turbines: A statistical model of motion maxima of offshore wind turbine components during installation (Version 1) [Data set and Codes]. `https://zenodo.org/record/5779878#.YdgtZS1XY1I`.

[18] Sander, A., 2020. Oscillations of Offshore Wind Turbines undergoing Installation I: Raw Measurements [Data set]. `https://zenodo.org/record/4141208#.Ydgtpy1XY1I`.

[19] Holman, B., 2021. “Hub motions of offshore wind turbines during single blade installation”. Master thesis, Delft University of Technology.

[20] Beirlant, J., Goegebeur, Y., Segers, J., and Teugels, J., 2004. *Statistics of Extremes*. John Wiley & Sons, Ltd, Chichester, England.

[21] Castillo, E., Hadi, A. S., Balakrishnan, N., and Sarabia, J. M., 2004. *Extreme Value and Related Models with Applications in Engineering and Science*, 1. ed. Wiley & Sons Ltd.

[22] Dimitrov, N., 2016. “Comparative analysis of methods for modelling the short-term probability distribution of extreme wind turbine loads”. *Wind Energy,* ***19***, pp. 717–737.

[23] Fogle, J., Agarwal, P., and Manuel, L., 2008. “Towards an improved understanding of statistical extrapolation for wind turbine extreme loads”. *Wind Energy,* ***11***(6), pp. 613–635.

[24] Mackay, E. B. L., and Jonathan, P., 2020. “Estimation of environmental contours using a block reampling method”. In Proceedings of the ASME 2020 39th International Conference on Ocean, Offshore & Arctic Engineering.

[25] Haselsteiner, A. F., Frieling, M., Mackay, E., Sander, A., and Thoben, K. D., 2022. “Long-term extreme response of an offshore turbine: How accurate are contour-based estimates?”. *Renewable Energy,* ***181***, pp. 945–965.

[26] Haselsteiner, A. F., Lehmkuhl, J., Pape, T., Windmeier, K.-L., and Thoben, K.-D., 2019. “ViroCon: A software to compute multivariate extremes using the environmental contour method”. *SoftwareX,* ***9***, pp. 95–101.